# Molecular orientation in uniaxial, one-way and two-way drawn poly(vinyl chloride) films

**I. Karacan, D. I. Bower* and I. M. Ward**
*IRC in Polymer Science and Technology, University of Leeds, Leeds LS2 9JT, UK*
*(Received 14 June 1993; revised 18 November 1993)*

Uniaxially oriented poly(vinyl chloride) films drawn at 90, 100 and 110°C to draw ratios in the range 1.5–3.5 have been investigated using i.r. spectroscopy and refractive index measurements. Their 10 s isochronal extensional creep moduli and dynamic tensile moduli have also been measured. One-way drawn films with draw ratios in the range $1.56 \times 1$–$2.56 \times 1$ and simultaneously and sequentially two-way drawn films with draw ratios in the range $1.46 \times 1.46$–$1.79 \times 1.79$ have been investigated using refractive index measurements and i.r. spectroscopy. These films were drawn at 85 and 95°C. Thermal analysis of the drawn samples showed that the uniaxially drawn films were drawn at temperatures well above their final glass transition temperatures, whereas the one-way and two-way drawn films were drawn close to their glass transition temperatures. The results show that the crystallites are more highly oriented than the amorphous chains and that one-way drawn samples depart slightly from uniaxiality. No significant difference in orientation was found between simultaneously and sequentially two-way drawn samples. It was shown that the i.r. peak at 613 $cm^{-1}$, attributed to short syndiotactic segments, could be used to characterize the orientation of the amorphous chains. The elastic moduli of the uniaxially drawn samples were found to depend on orientation in a similar way to that previously reported.

**(Keywords: poly(vinyl chloride); orientation; infra-red spectroscopy)**

## INTRODUCTION

During the past few decades, poly(vinyl chloride) (PVC) has been widely used in the packaging industry for producing bottles and films, because of its desirable optical and mechanical properties. It is well understood that uniaxial drawing enhances the properties of polymers in the direction of drawing; however, the properties in the perpendicular direction remain relatively impaired. On the other hand, biaxial drawing improves the properties of polymers in both directions and hence results in enhanced properties in the plane of the samples, so that in recent years there has been an increasing interest in the production of one-way and two-way (biaxially) drawn PVC films and tubes[1].

The structure and properties of uniaxially oriented PVC have been the subject of many investigations using methods such as Raman spectroscopy[2–4], i.r. spectroscopy[5–7], n.m.r.[8], and X-ray diffraction[9,10]. In particular, Robinson *et al.*[2] used Raman spectroscopy in the C–Cl stretching region and birefringence measurements to obtain orientational information on uniaxially oriented PVC, and showed that the crystallites were more highly oriented than the non-crystalline material in samples containing higher amounts of plasticizer drawn at higher temperatures. Subsequently, Bower *et al.*[3] used the intensity of the 616 $cm^{-1}$ Raman peak, specific for short syndiotactic sequences, to deduce that the amorphous chains behave in a rubber-like way during orientation.

King *et al.*[4] studied the effect of plasticizer content on the orientation and mechanical properties of uniaxially oriented PVC and found that the presence of plasticizer resulted in lower moduli. This conclusion was attributed to the diluent effect of the plasticizer on the load-bearing chains. The Raman measurements suggested that the crystallites orient rather like rigid rods in an affinely deforming matrix, with some relaxation.

In addition to Raman spectroscopy, broad-line n.m.r. spectroscopy has been utilized to characterize the orientation of uniaxially oriented PVC films. In one such study Kashiwagi and Ward[8] studied PVC samples with rather low orientation and obtained orientation averages that were consistent with those obtained by other methods, even though they assumed very simple molecular conformations.

Traditionally, X-ray diffraction analysis has been employed to characterize crystallite orientation and the degree of crystallinity of semicrystalline polymers with reasonably high crystallinity values, where the X-ray diffraction patterns reveal well defined crystalline reflections. Such studies are difficult for PVC because of its inherent low crystallinity and the complicated nature of the amorphous background scattering, but some work has been undertaken.

Gilbert and co-workers[9,10] studied the structural changes taking place upon drawing using thermal and X-ray diffraction analyses. Vyvoda *et al.*[9] investigated the effects of uniaxial drawing and annealing on the tensile properties of rigid PVC, and explained the observed behaviour in terms of structural changes detected by X-ray diffraction. They showed that low temperature drawing led to a reduction in three-dimensional order and an increase in two-dimensional order. It was shown that the maximum two-dimensional order occurred on

* To whom correspondence should be addressed

0032-3861/94/16/3411-12

annealing at 110°C and that the mechanical anisotropy in terms of tensile yield stress decreased following annealing. In a recent study, Liu and Gilbert[10] investigated the possibility of enhancing the mechanical properties of heavily plasticized PVC compounds by monitoring the effects produced by a variety of drawing and annealing treatments using X-ray diffraction analysis. Their results showed that the ultimate strength of drawn and annealed samples increased in the draw direction and that the elongation to break decreased. They attributed these improvements to the development of two-dimensional structural order perpendicular to the chain direction.

With few exceptions, biaxial drawing of PVC films has not been the subject of detailed investigation and the published literature is mainly concerned with the production and mechanical properties of the films. No detailed characterization of orientation in biaxially oriented PVC films has been reported so far.

The most extensive information concerned with the relationship between stretching conditions and resultant properties was published by Brady[11] and de Vries and Bonnebat[12]. Brady[11] investigated the influence of the degree of biaxial orientation, stretching rate and stretching temperature on the tensile, dynamic mechanical and dielectric properties, and showed that a $2 \times 2$ stretch ratio is optimum for impact resistance. De Vries and Bonnebat[12] examined the stretching of PVC and chlorinated PVC with a view to understanding their behaviour in thermoforming processes. Optimum forming conditions were identified and the effect of biaxial orientation on various properties, such as dimensional stability, impact resistance and gas permeability, was also reported. Sakaguchi and Nagano[13,14] reported an analysis of the tensile behaviour of biaxially oriented plasticized PVC sheet using finite element analysis. Recently, Gilbert and Liu[15] studied the effect of biaxial orientation on plasticized and unplasticized PVC. They examined the tensile properties of biaxially oriented samples and used X-ray diffraction to investigate the development of structural order. They also showed that biaxial stretching produced significant property changes in both plasticized and unplasticized samples. Selwood *et al.*[1] produced thick-walled biaxially oriented PVC tubes using a die-drawing technique, and showed that the tensile strength and extensibility of biaxially drawn tubes can be considerably enhanced.

The present paper describes the characterization of uniaxial, one-way (constant width) and two-way drawn PVC films using i.r. spectroscopy, refractive index measurements, thermal analysis and static and dynamic mechanical measurements, with the aim of understanding the development of orientation under a wide variety of drawing conditions.

## EXPERIMENTAL

### *Materials*

The drawn PVC films were prepared from Staufen type 48.4 commercial PVC sheet of thickness 80 $\mu$m, produced by ICI plc. This material contains about 5–10% vinyl acetate and a few per cent of additives such as stabilizers and lubricants, but no plasticizer. The total amount of additives was estimated to be about 15% and this figure has been used in correcting the infra-red spectra of the samples investigated.

### *Preparation of uniaxially drawn films*

The uniaxially oriented samples were drawn in a hot air oven on an Instron tensile testing machine at a crosshead speed of 25 mm min$^{-1}$, and at draw temperatures of 90, 100 and $110 \pm 1$°C. These samples were cut from commercially available A4 size sheets; the gauge length was 60 mm and the width 20 mm. As soon as the required draw ratio was reached the oven door was

**Table 1** Sample details for uniaxially oriented PVC films

| Draw ratio, $\lambda$ | Draw temp. (°C) | Refractive indices | | Birefringence, $\Delta n \times 10^{-3}$ | Density (g cm$^{-3}$) | $T_g$ (°C) |
|---|---|---|---|---|---|---|
| | | $n_M$ | $n_T$ | | | |
| 1.00 | 90 | 1.5384 | 1.5380 | 0.4 | 1.3358 | 76.0 |
| 1.47 | 90 | 1.5393 | 1.5378 | 1.5 | 1.3367 | 77.1 |
| 1.95 | 90 | 1.5399 | 1.5367 | 3.2 | 1.3371 | 78.1 |
| 2.44 | 90 | 1.5409 | 1.5367 | 4.2 | 1.3374 | 79.6 |
| 2.95 | 90 | 1.5411 | 1.5363 | 4.8 | 1.3373 | 80.7 |
| 3.37 | 90 | 1.5424 | 1.5365 | 5.9 | 1.3375 | 81.4 |
| 1.00 | 100 | 1.5397 | 1.5394 | 0.3 | 1.3368 | 75.0 |
| 1.47 | 100 | 1.5406 | 1.5393 | 1.3 | 1.3370 | 76.1 |
| 1.89 | 100 | 1.5413 | 1.5386 | 2.7 | 1.3380 | 77.1 |
| 2.47 | 100 | 1.5424 | 1.5384 | 4.0 | 1.3387 | 78.8 |
| 2.95 | 100 | 1.5424 | 1.5380 | 4.4 | 1.3393 | 80.1 |
| 3.58 | 100 | 1.5431 | 1.5376 | 5.5 | 1.3394 | 80.9 |
| 1.00 | 110 | 1.5398 | 1.5396 | 0.2 | 1.3387 | 74.5 |
| 1.47 | 110 | 1.5404 | 1.5392 | 1.2 | 1.3400 | 75.8 |
| 2.05 | 110 | 1.5407 | 1.5382 | 2.5 | 1.3407 | 76.8 |
| 2.47 | 110 | 1.5426 | 1.5393 | 3.3 | 1.3411 | 78.2 |
| 2.95 | 110 | 1.5427 | 1.5387 | 4.0 | 1.3413 | 79.3 |
| 3.20 | 110 | 1.5434 | 1.5390 | 4.4 | 1.3414 | 79.8 |

opened and the sample was allowed to cool to just above room temperature in about 60 s. The draw was found to be homogeneous and very closely uniaxial, as shown by the changes in the width and the thickness directions. The draw ratios of uniaxially oriented samples are shown in *Table 1*.

*Preparation of one-way and two-way drawn films*

The one-way (constant width) and two-way drawn samples were drawn in a novel biaxial testing machine designed and constructed in the IRC laboratory, in which plane sheets can be drawn in two perpendicular directions within a high-temperature oven under isothermal conditions with independent control of draw speed in the two directions. The samples were cut from material in the form of commercially available rolls and were initially squares of size 190 × 190 mm. The drawing experiments were carried out at 85 and 95 ± 1°C at a drawing speed of 60 mm $min^{-1}$. The draw ratios of the constant width and two-way drawn samples are shown in *Table 2*. The subscripts M and T stand for 'machine' and 'transverse' directions within the plane of the film. The machine direction always coincides with the roll-off direction of the original film. In one-way constant width drawing this was always the draw direction and the width of the sample was constrained to remain unchanged in the transverse direction. In sequential two-way drawing the first drawing was one-way in this sense and the second draw was thus in the transverse direction.

*Density measurements*

Density measurements were carried out with a graded density column obtained from mixtures of potassium iodide and distilled water to give a density range of 1.22–1.42 g $cm^{-3}$. The densities are accurate to about $\pm 1 \times 10^{-4}$ and are presented in *Tables 1* and *2*.

*Refractive index measurements*

Refractive index measurements were carried out with a Bellingham and Stanley Abbe refractometer using α-bromonaphthalene as the optical contact liquid. The measured refractive indices in the transverse and normal directions were equal for uniaxially oriented samples within the experimental uncertainty of $\pm 1 \times 10^{-4}$, which confirmed the uniaxiality of the samples. The birefringence of a uniaxially oriented polymer film is the difference ($\Delta n$) between the refractive index for light polarized parallel to the draw (machine) direction, $n_M$, and that for light polarized perpendicular to the draw direction, $n_T$. The measured values of the refractive indices and the birefringences for uniaxially oriented samples are shown in *Table 1* and the birefringences are plotted against draw ratio in *Figure 1*. The measured values of refractive indices for constant width and two-way drawn samples are shown in *Table 2*.

*D.s.c. measurements*

The differential scanning calorimetry experiments were carried out using a Perkin–Elmer DSC7 instrument at a heating rate of 10°C $min^{-1}$. Small samples were cut from undrawn and drawn films to fit in porous aluminium pans. Typical sample weights used were in the range 8–9 mg. The calorimeter was adjusted to give a flat baseline over the temperature of interest, 5–175°C. The glass transition temperatures, $T_g$, were evaluated using the Perkin–Elmer thermal analysis data system and were defined as the temperature of the maximum in the first

**Table 2** Sample details for constant width and two-way drawn PVC films

| Draw ratio, $\lambda_M \times \lambda_T$ | Draw temp. (°C) | Refractive indices | | | Density (g $cm^{-3}$) | $T_g$ (°C) |
|---|---|---|---|---|---|---|
| | | $n_M$ | $n_T$ | $n_N$ | | |
| One-way drawn samples | | | | | | |
| 1.00 × 1.00 | 85 | 1.5398 | 1.5393 | 1.5392 | 1.3530 | 83.9 |
| 1.56 × 1.00 | 85 | 1.5412 | 1.5393 | 1.5392 | 1.3531 | 85.1 |
| 1.79 × 1.00 | 85 | 1.5417 | 1.5393 | 1.5387 | 1.3532 | 85.6 |
| 2.01 × 1.00 | 85 | 1.5420 | 1.5392 | 1.5386 | 1.3533 | 85.9 |
| 2.56 × 1.00 | 85 | 1.5428 | 1.5392 | 1.5384 | 1.3538 | 86.6 |
| 1.00 × 1.00 | 95 | 1.5399 | 1.5394 | 1.5393 | 1.3535 | 83.4 |
| 1.51 × 1.00 | 95 | 1.5414 | 1.5394 | 1.5393 | 1.3538 | 84.6 |
| 1.75 × 1.00 | 95 | 1.5417 | 1.5394 | 1.5388 | 1.3540 | 85.0 |
| 1.93 × 1.00 | 95 | 1.5420 | 1.5394 | 1.5387 | 1.3542 | 85.5 |
| 2.38 × 1.00 | 95 | 1.5425 | 1.5393 | 1.5385 | 1.3546 | 86.0 |
| Simultaneously biaxially drawn samples | | | | | | |
| 1.53 × 1.53 | 85 | 1.5407 | 1.5399 | 1.5386 | 1.3547 | 86.0 |
| 1.79 × 1.79 | 85 | 1.5410 | 1.5406 | 1.5384 | 1.3539 | 84.9 |
| 1.46 × 1.47 | 95 | 1.5411 | 1.5407 | 1.5389 | 1.3546 | 85.7 |
| 1.66 × 1.70 | 95 | 1.5415 | 1.5408 | 1.5390 | 1.3541 | 84.3 |
| Sequentially biaxially drawn samples | | | | | | |
| 1.53 × 1.53 | 85 | 1.5410 | 1.5401 | 1.5385 | 1.3551 | 85.9 |
| 1.79 × 1.79 | 85 | 1.5412 | 1.5402 | 1.5384 | 1.3546 | 85.5 |
| 1.51 × 1.51 | 95 | 1.5411 | 1.5401 | 1.5385 | 1.3551 | 85.7 |
| 1.64 × 1.64 | 95 | 1.5415 | 1.5407 | 1.5386 | 1.3540 | 85.3 |

derivative of the d.s.c. scan (see *Figure 2*). Indium (m.p. 156.5°C) and zinc (m.p. 419.5°C) were used as calibration standards. The specimens were always tested in a nitrogen environment. The glass transition temperatures are accurate to ±0.3°C and are listed in *Tables 1* and *2*.

*Mechanical measurements*

Two types of macroscopic mechanical extensional moduli were measured for the uniaxial samples: (1) the 10 s isochronal creep modulus, which can be readily compared with earlier measurements of extensional moduli on similar samples; (2) the dynamic modulus, which provides information about molecular mobility. The values of the moduli are shown in *Table 3*.

*Isochronal extensional modulus measurements.* Strips of material, 2 mm wide and 60 mm long, were cut parallel to the draw direction. The extensional moduli were measured using a modified form of the dead-loading extensional creep apparatus of Gupta and Ward[16]. Each sample was mechanically conditioned before readings were taken, by cycles of loading for 10 s and relaxation for 110 s. Any distortion of the apparatus as a whole was removed by suitable calibration[17].

*Dynamic modulus.* Dynamic extensional moduli were measured as a function of frequency in the range 1–100 rad $s^{-1}$ and in the temperature range −90 to 90°C using a Rheometrics RSA2 solids analyser. Strip samples, 2 mm wide and ~24 mm long, were mounted between specially designed film/fibre grips with the long axes positioned in the vertical direction. A sinusoidal extension was applied to the sample by means of a vibrator, and the resulting force induced in the sample was measured by a force transducer. The measurements were carried out inside a thermally insulated enclosure and nitrogen gas was used to control the temperature of the samples. The measurements were carried out with the samples under a dead load sufficient to produce a static strain of about 0.25% in the linear region of the stress–strain curves, and the oscillatory strain was held constant at 0.2%.

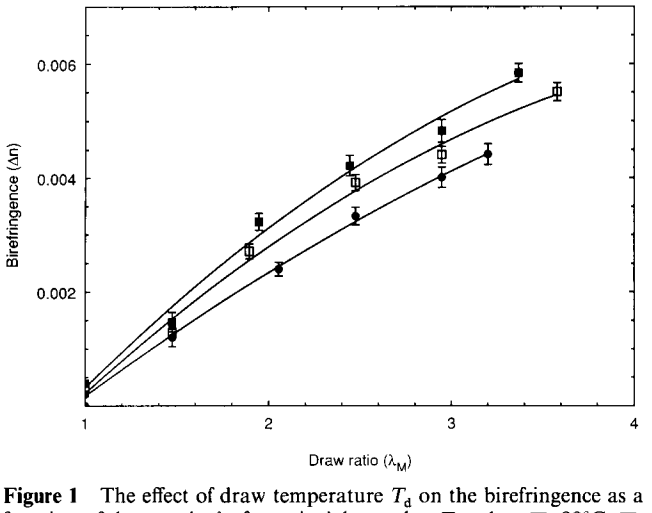


**Figure 1** The effect of draw temperature $T_d$ on the birefringence as a function of draw ratio $\lambda_M$ for uniaxial samples. $T_d$ value: ■, 90°C; □, 100°C; ●, 110°C

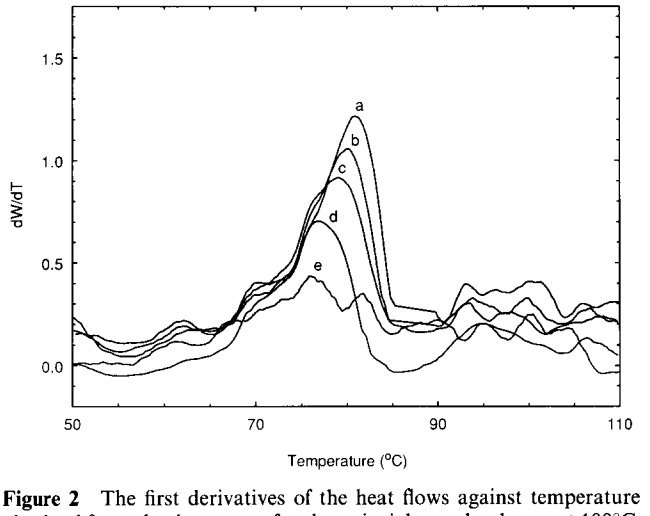


**Figure 2** The first derivatives of the heat flows against temperature obtained from the d.s.c. scans for the uniaxial samples drawn at 100°C. Value of $\lambda$: (a) 3.58; (b) 2.95; (c) 2.47; (d) 1.89; (e) 1.47

**Table 3** Extensional modulus results for uniaxially oriented PVC films

| Draw ratio, $\lambda$ | Draw temp. (°C) | 10 s creep modulus at room temp. (GPa) | Dynamic modulus (GPa) at 100 rad $s^{-1}$ and | | | |
|---|---|---|---|---|---|---|
| | | | −80°C | 0°C | 20°C | 60°C |
| 1.47 | 90 | 3.26 | 6.25 | 4.18 | 3.80 | 2.62 |
| 1.95 | 90 | 3.51 | 6.57 | 4.60 | 4.24 | 2.99 |
| 2.44 | 90 | 4.13 | 7.74 | 5.38 | 4.94 | 3.52 |
| 2.95 | 90 | 4.63 | 8.19 | 6.30 | 5.81 | 4.16 |
| 3.37 | 90 | 4.99 | 9.39 | 7.00 | 6.45 | 4.69 |
| 1.47 | 100 | 3.23 | 5.97 | 4.25 | 3.92 | 2.71 |
| 1.89 | 100 | 3.71 | 6.60 | 4.66 | 4.31 | 3.00 |
| 2.47 | 100 | 4.24 | 8.18 | 5.62 | 5.16 | 3.81 |
| 2.95 | 100 | 4.64 | 8.43 | 5.96 | 5.48 | 4.00 |
| 3.58 | 100 | 5.18 | 9.04 | 6.42 | 5.91 | 4.28 |
| 1.47 | 110 | 3.13 | 6.00 | 4.04 | 3.70 | 2.47 |
| 2.05 | 110 | 3.42 | 6.35 | 4.49 | 4.15 | 2.82 |
| 2.47 | 110 | 3.88 | 7.21 | 5.10 | 4.64 | 3.28 |
| 2.95 | 110 | 4.28 | 8.24 | 5.86 | 5.36 | 3.85 |
| 3.20 | 110 | 4.61 | 9.12 | 6.55 | 6.03 | 4.39 |

*Infra-red measurements*

A Nicolet 740 Fourier transform infra-red spectrophotometer equipped with a KRS5-based wire grid polarizer positioned adjacent to the sample was employed for i.r. dichroic measurements, the beam passing first through the polarizer and then through the sample before reaching the detector. The polarizer remained in a fixed orientation throughout and the samples were rotated in order to obtain spectra for different polarization directions. The method used to obtain the 'normal' and 'tilted-film' spectra required for the characterization of orientation in films that do not have uniaxial symmetry has been described in detail previously[18].

In all cases, 100 interferograms of a sample were averaged and transformed with Happ-Genzel apodization function. Each sample spectrum was ratioed against a corresponding number of background scans using the same polarizer and instrument settings. The specimen chamber was purged to minimize water vapour and carbon dioxide in the air. All the spectra were collected at a resolution of 1 $cm^{-1}$. Finally, all the i.r. data were transferred to an Amdahl mainframe computer for analysis.

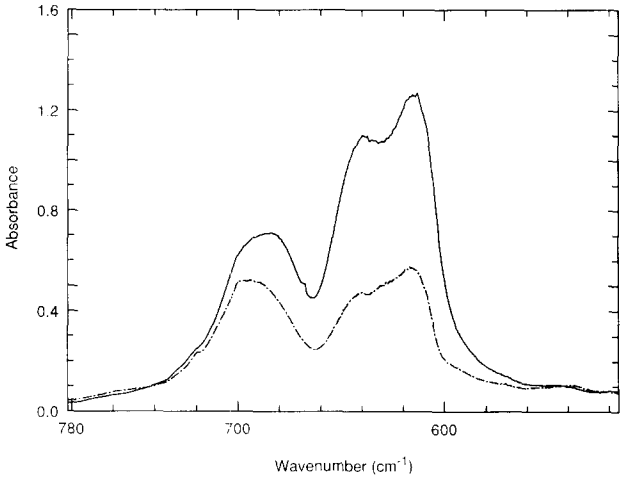


**Figure 3** The i.r. spectrum of uniaxially oriented PVC film in the C–Cl stretching region (500–790 $cm^{-1}$); draw temperature $T_d = 90°C$, draw ratio $\lambda = 3.37$. ——, Perpendicular polarization; —· —·, parallel polarization

Since the direction of vibration of the C–Cl bond in the stretching mode is approximately perpendicular to the main chain, which tends to align parallel to the draw direction, the intensity of the i.r. spectrum in the C–Cl stretching region (500–790 $cm^{-1}$) is stronger for the perpendicular polarization direction than for the parallel polarization direction, as shown in *Figure 3*.

The directly measured absorbance values were subject to errors, because the polarizer transmits a small fraction of radiation polarized perpendicularly to its principal transmission direction. These errors were corrected according to a procedure developed by Green and Bower[19]. The corrections were found to be small for samples of high draw ratios and insignificant for samples with low draw ratios, for which the true absorbance values in both directions are similar. As already mentioned, the samples under investigation contain about 15% of additives. The i.r. spectrum of undrawn pure PVC (BP product) in the 500–790 $cm^{-1}$ region was normalized in order to take into account the effect of film thickness, and 85% of this spectrum was subtracted from the spectrum of an unoriented sample of the ICI PVC. The difference spectrum was taken to be the spectrum of the additives and was subtracted from the spectra of the oriented PVC samples, again normalized in order to take into account the effect of film thickness. This correction assumes that the orientation of the additives is not significant.

## DATA ANALYSIS

*Infra-red data – curve fitting*

Previous studies of the C–Cl stretching region of PVC by Raman[2,3] and i.r.[6] spectroscopy have shown that the region 600–650 $cm^{-1}$ can be fitted with six Lorentzian peaks. The earlier studies suggested that the region 650–720 $cm^{-1}$ can be fitted with two[6] or three[2,3] peaks, but more recent studies[20,21] have shown that this region can best be fitted with four Lorentzian peaks. The curve fitting of the Raman spectrum by Robinson *et al.*[2] showed that the peaks in the 600–650 $cm^{-1}$ region have widths (full width at half peak intensity) in the range 12–20 $cm^{-1}$, whereas the peaks in the 650–710 $cm^{-1}$ region have widths between 24 and 34 $cm^{-1}$. According to Maddams and Tooke[22], widths in the range 14–22 $cm^{-1}$ were found for the 600–650 $cm^{-1}$ region of

**Table 4** Assignment of PVC absorption peaks in the 500–790 $cm^{-1}$ region

| Infra-red | | Present study | Raman[20,21] | Configuration[20] | Conformation[6,21] |
|---|---|---|---|---|---|
| Ref. 28 | Ref. 29 | | | | |
| 603 | 605 | 606.6 | 607.9 | S[a] | crystalline all-*trans* |
| 613 | 614 | 613.0 | 614.5 | S | *TTTT* short *trans* |
| 624 | 623 | 621.8 | 622.0 | I | |
| 633 | 635 | 632.5 | 629.5 | S | |
| 639 | 638 | 638.9 | 636.4 | S | crystalline all-*trans* |
| 647 | 647 | 647.9 | 645.7 | H | |
| 677 | 681 | 677.2 | 676.7 | I or H | |
| | | 689.1 | 688.7 | H | |
| 695 | 698 | 696.9 | 697.6 | I | *TGTGTG* isotactic helix |
| | | 706.2 | 707.3 | H | |

[a] S, syndiotactic triad; I, isotactic triad; H, heterotactic triad

the i.r. spectrum, whereas the widths were between 25 and 29 $cm^{-1}$ for the 650–700 $cm^{-1}$ region. *Table 4* shows the peak positions found in several studies, together with some of the assignments.

In the present work the parallel and perpendicular polarization spectra of uniaxially oriented samples were first fitted independently, allowing the peak positions and widths to vary freely, using the positions and widths previously found as a guide to starting values. Finally, the peak positions and the widths obtained from all the spectra were averaged and the parallel and the perpendicular spectra were refitted, fixing the positions and the widths at these average values and allowing only the peak heights to vary. The use of six Lorentzian peaks in the 600–650 $cm^{-1}$ region and four Lorentzian peaks in the 650–720 $cm^{-1}$ region was found to give good fits to the spectra. In addition to the major peaks, seven minor peaks were required at 496, 514, 540, 553, 573, 586 and 592 $cm^{-1}$ to improve the fits in the tails of the major peaks, but they are not considered further. An example of the curve fitting is shown in *Figure 4*. The same curve fitting procedure was utilized for the spectra corresponding to the constant width and two-way drawn samples.

*Infra-red data – evaluation of orientation averages*

If we know the orientation of the transition moment within the structural unit for a particular i.r. absorption and measure the peak absorbances for polarization parallel to the machine, transverse and normal directions, orientation averages of the structural units with respect to the sample axes can be calculated, provided that certain assumptions are made[23].

The dichroic ratio, $D$, for a uniaxially oriented sample, is defined as:

$$D = A_{\parallel}/A_{\perp} \tag{1}$$

where $A_{\parallel}$ and $A_{\perp}$ are the measured absorbances for radiation polarized parallel and perpendicular to the draw direction, respectively. To a good approximation, the dichroic ratio, $D$, is related to the orientation average $\langle P_2(\cos\theta)\rangle$ by:

$$\langle P_2(\cos\theta)\rangle = \frac{1}{2}\langle 3\cos^2\theta - 1\rangle = \frac{D-1}{D+2}\frac{D_0+2}{D_0-1} \tag{2}$$

where $\theta$ is the angle between the molecular axis and the draw direction, and $D_0 = 2\cot^2\alpha$, $\alpha$ being the angle between the transition moment associated with the

**Table 5** Second moment averages of uniaxially oriented samples drawn at 100°C as measured by i.r. spectroscopy

| Draw ratio, $\lambda$ | $\langle P_2(\cos\theta)\rangle$ Corrected for polarizer only | $\langle P_2(\cos\theta)\rangle$ Corrected for polarizer and 15% additives |
|---|---|---|
| | $\tilde{\nu} = 606.2\ cm^{-1}$ | $\tilde{\nu} = 606.6\ cm^{-1}$ |
| 1.47 | 0.30 | 0.41 |
| 1.89 | 0.41 | 0.55 |
| 2.47 | 0.56 | 0.75 |
| 2.95 | 0.60 | 0.82 |
| 3.58 | 0.67 | 0.93 |
| | $\tilde{\nu} = 613.3\ cm^{-1}$ | $\tilde{\nu} = 613.0\ cm^{-1}$ |
| 1.47 | 0.14 | 0.14 |
| 1.89 | 0.20 | 0.23 |
| 2.47 | 0.29 | 0.28 |
| 2.95 | 0.35 | 0.35 |
| 3.58 | 0.39 | 0.38 |
| | $\tilde{\nu} = 638.8\ cm^{-1}$ | $\tilde{\nu} = 638.9\ cm^{-1}$ |
| 1.47 | 0.18 | 0.21 |
| 1.89 | 0.29 | 0.35 |
| 2.47 | 0.44 | 0.51 |
| 2.95 | 0.46 | 0.58 |
| 3.58 | 0.56 | 0.67 |
| | $\tilde{\nu} = 688.4\ cm^{-1}$ | $\tilde{\nu} = 689.0\ cm^{-1}$ |
| 1.47 | 0.06 | 0.06 |
| 1.89 | 0.10 | 0.11 |
| 2.47 | 0.13 | 0.14 |
| 2.95 | 0.15 | 0.16 |
| 3.58 | 0.17 | 0.18 |

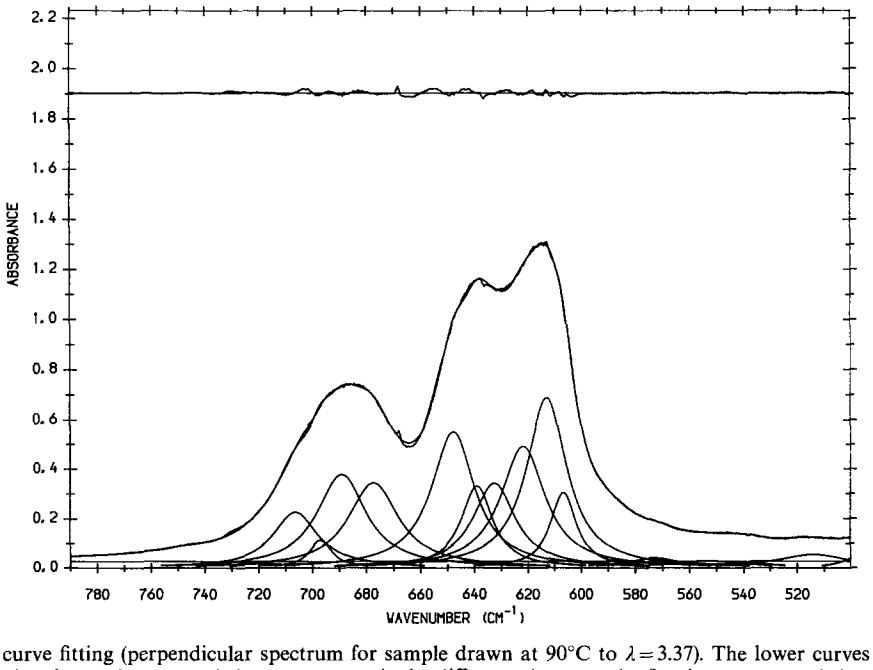


**Figure 4** An example of curve fitting (perpendicular spectrum for sample drawn at 90°C to $\lambda = 3.37$). The lower curves are the fitted Lorentzian peaks, the middle curve is the observed curve and the upper curve is the difference between the fitted spectrum and the observed spectrum on the same scale

vibrational mode and the molecular axis. It is assumed that the chains have no preferred orientation around their own axes. A full treatment of the determination of orientation averages from i.r. data is given by Cunningham *et al.*[24,25]. This treatment includes corrections due to reflections from the sample surfaces and the internal field effect. However, for samples with very low birefringence, such as the present samples, equations (1) and (2) are sufficiently accurate. The values of $\langle P_2(\cos\theta)\rangle$ found using the peaks at 607, 613, 639 and 689 $cm^{-1}$, assuming $\alpha = 90°$, are presented in *Table 5* for the samples drawn at 100°C. Values obtained from spectra corrected only for polarizer imperfections and values obtained from spectra corrected for both polarizer imperfections and 15% additives, are given for comparison. *Table 6* shows values obtained from fully corrected spectra for all uniaxial samples.

In the present study, the procedure described by Jarvis *et al.*[23] was used for analysing the i.r. data of one-way (constant width) and two-way drawn samples. In this analysis the values of the imaginary parts $k_i$ of the three complex refractive indices $n_i - ik_i$ at each absorption peak are first calculated, where $i = M$, T or N. The orientation parameters are then evaluated from $k_i$ and $n_i$, with the values of $n_i$ approximated by the optical refractive indices. The steps in the calculation have been listed explicitly in reference 18.

The orientation averages $P_{2mn}$ (see references 18 and 23) are given by:

$$\frac{2\phi_M - \phi_T - \phi_N}{\phi_M + \phi_T + \phi_N} = 2p_{200}(\theta_m)P_{200} + 4p_{200}(\theta_m)P_{202} - 4P_{202} \tag{3}$$

$$\frac{\phi_T - \phi_N}{\phi_M + \phi_T + \phi_N} = 4p_{200}(\theta_m)P_{220} + \frac{4}{3}p_{200}(\theta_m)P_{222} - \frac{4}{3}P_{222} \tag{4}$$

where $\phi_i = 6n_i k_i/(n_i^2 + 2)^2$ with $i = N$, M or T, $\theta_m$ is the angle between the chain axis and the transition moment for a particular vibrational mode and $p_{200}(\theta_m) = P_2(\cos\theta_m)$.

The transition moment angles for the C–Cl stretching peaks at 607, 613, 639 and 689 $cm^{-1}$ were assumed to be 90°, and for these peaks equations (1) and (2) reduce to:

$$\frac{2\phi_M - \phi_T - \phi_N}{\phi_M + \phi_T + \phi_N} = -(P_{200} + 6P_{202}) \quad \text{for } \theta_m = 90° \tag{5}$$

$$\frac{\phi_T - \phi_N}{\phi_M + \phi_T + \phi_N} = -2(P_{220} + P_{222}) \quad \text{for } \theta_m = 90° \tag{6}$$

If it is assumed that there is no preferential orientation of chains around the chain axis, the values of $P_{202}$ and $P_{222}$ may be set to zero, so that:

$$\frac{2\phi_M - \phi_T - \phi_N}{\phi_M + \phi_T + \phi_N} = -P_{200} \quad \text{for } \theta_m = 90°,\ P_{202} = 0 \tag{7}$$

$$\frac{\phi_T - \phi_N}{\phi_M + \phi_T + \phi_N} = -2P_{220} \quad \text{for } \theta_m = 90°,\ P_{222} = 0 \tag{8}$$

Equations (7) and (8) were used to calculate the values of $P_{200}$ and $P_{220}$ for the peaks at 607, 613, 639 and 689 $cm^{-1}$. The corresponding values of $\langle\cos^2\theta_{c,i}\rangle$, where $i = M$, T or N, and $\theta_{c,i}$ is the angle between the chain axis and the $i$ direction, are given by the equations[23]:

$$\langle\cos^2\theta_{c,M}\rangle = \frac{1}{3} + \frac{2}{3}P_{200} \tag{9}$$

$$\langle\cos^2\theta_{c,T}\rangle = \frac{1}{3} - \frac{1}{3}P_{200} + 2P_{220} \tag{10}$$

$$\langle\cos^2\theta_{c,N}\rangle = \frac{1}{3} - \frac{1}{3}P_{200} - 2P_{220} \tag{11}$$

Values of $\langle\cos^2\theta_{c,i}\rangle$ for the one-way and two-way drawn samples deduced from data for the peaks at 613 and 639 $cm^{-1}$ are given in *Table 7*.

**Table 6** Second moment averages of uniaxially oriented samples as measured by i.r. spectroscopy (corrected for polarizer imperfections and 15% additives)

| Draw ratio, $\lambda$ | Draw temp. (°C) | $\langle P_2(\cos\theta)\rangle$ Crystalline 607 $cm^{-1}$ | Crystalline 639 $cm^{-1}$ | Amorphous 613 $cm^{-1}$ | Amorphous 689 $cm^{-1}$ | Cystallinity (i.r.) (%) |
|---|---|---|---|---|---|---|
| 1.47 | 90 | 0.16 | 0.16 | 0.17 | 0.08 | 11.5 |
| 1.95 | 90 | 0.35 | 0.26 | 0.23 | 0.12 | 11.5 |
| 2.44 | 90 | 0.52 | 0.37 | 0.32 | 0.14 | 11.2 |
| 2.95 | 90 | 0.64 | 0.45 | 0.38 | 0.17 | 9.9 |
| 3.37 | 90 | 0.80 | 0.56 | 0.42 | 0.18 | 9.6 |
| 1.47 | 100 | 0.41 | 0.21 | 0.14 | 0.06 | 13.8 |
| 1.89 | 100 | 0.55 | 0.35 | 0.23 | 0.11 | 13.6 |
| 2.47 | 100 | 0.75 | 0.51 | 0.28 | 0.14 | 13.6 |
| 2.95 | 100 | 0.82 | 0.58 | 0.35 | 0.16 | 12.4 |
| 3.58 | 100 | 0.93 | 0.67 | 0.38 | 0.18 | 12.2 |
| 1.47 | 110 | 0.46 | 0.24 | 0.07 | 0.05 | 15.0 |
| 2.05 | 110 | 0.63 | 0.40 | 0.18 | 0.10 | 14.7 |
| 2.47 | 110 | 0.78 | 0.52 | 0.24 | 0.12 | 14.3 |
| 2.95 | 110 | 0.93 | 0.67 | 0.29 | 0.15 | 14.2 |
| 3.20 | 110 | 0.98 | 0.70 | 0.30 | 0.16 | 13.8 |

*Evaluation of orientation averages from refractive indices*

The measured refractive indices can be used to calculate orientation averages for the samples by using the following general equations[23]:

$$\frac{2\phi_M^e-\phi_T^e-\phi_N^e}{\phi_M^e+\phi_T^e+\phi_N^e}=\frac{2\Delta\alpha}{3\alpha_0}P_{200}+\frac{2\delta\alpha}{\alpha_0}P_{202} \quad (12)$$

$$\frac{\phi_T^e-\phi_N^e}{\phi_M^e+\phi_T^e+\phi_N^e}=\frac{4\Delta\alpha}{3\alpha_0}P_{220}+\frac{2\delta\alpha}{3\alpha_0}P_{222} \quad (13)$$

where

$$\phi_i^e=\frac{n_i^2-1}{n_i^2+2} \quad (14)$$

Here

$$\alpha_0=\frac{1}{3}(\alpha_1+\alpha_2+\alpha_3) \quad (15)$$

$$\Delta\alpha=\alpha_3-(\alpha_1+\alpha_2)/2 \quad (16a)$$

and

$$\delta\alpha=(\alpha_1-\alpha_2) \quad (16b)$$

where $\alpha_1$, $\alpha_2$ and $\alpha_3$ are the principal components of the electronic polarizability tensor for a unit. The $Ox_3$ axis of the unit is assumed to be parallel to the chain axis. Assuming, as above, that there is no preferential orientation of chains around their own axes, the values of $P_{202}$ and $P_{222}$ may be set to zero and equations (12) and (13) reduce to:

$$\frac{2\phi_M^e-\phi_T^e-\phi_N^e}{\phi_M^e+\phi_T^e+\phi_N^e}=\frac{2\Delta\alpha}{3\alpha_0}P_{200} \quad (17)$$

$$\frac{\phi_T^e-\phi_N^e}{\phi_M^e+\phi_T^e+\phi_N^e}=\frac{4\Delta\alpha}{3\alpha_0}P_{220} \quad (18)$$

For PVC the three refractive indices differ from their mean value by $<10^{-2}$. Substituting the expressions for $\phi_i$ from equation (14) into equations (17) and (18) and writing $\Delta n=n_M-(n_T+n_N)/2$ and $\Delta n_{TN}=n_T-n_N$ then leads, to a good approximation, to:

$$P_{200}=\left(\frac{3\alpha_0}{\Delta\alpha}\right)\frac{2n_0\Delta_n}{(n_0^4+n_0^2-2)} \quad (19)$$

$$P_{220}=\left(\frac{3\alpha_0}{\Delta\alpha}\right)\frac{n_0\Delta n}{2(n_0^4+n_0^2-2)} \quad (20)$$

where $n_0=\frac{1}{3}(n_M+n_T+n_N)$ has been substituted for $n_M$, $n_T$ and $n_N$ in terms not involving a difference of refractive indices. It will be shown later that the maximum birefringence for a fully uniaxially oriented sample of PVC is $12.5\times10^{-3}$. Substituting $P_{200}=1$ in equation (19), together with the experimental value of $n_0$, leads to $3\alpha_0/\Delta\alpha=156\pm2$. Using this value and equations (19) and (20), the values of $P_{200}$ and $P_{220}$ can be determined from the refractive index data shown in *Tables 1* and *2*. From $P_{200}$ and $P_{220}$ the values of $\langle\cos^2\theta_{c,i}\rangle_{opt}$ can be

**Table 7** Values of $\langle\cos^2\theta_{c,i}\rangle$ for machine, transverse and normal directions for constant width one-way and two-way drawn samples

| Draw ratio | $\langle\cos^2\theta_{c,M}\rangle$ | | | $\langle\cos^2\theta_{c,T}\rangle$ | | | $\langle\cos^2\theta_{c,N}\rangle$ | | |
|---|---|---|---|---|---|---|---|---|---|
| | 613 $cm^{-1}$ | Opt. | 639 $cm^{-1}$ | 613 $cm^{-1}$ | Opt. | 639 $cm^{-1}$ | 613 $cm^{-1}$ | Opt. | 639 $cm^{-1}$ |
| One-way drawn samples (drawn at 85°C) | | | | | | | | | |
| 1.56 × 1.0 | 0.48 | 0.44 | 0.57 | 0.26 | 0.29 | 0.30 | 0.26 | 0.28 | 0.13 |
| 1.79 × 1.0 | 0.50 | 0.48 | 0.60 | 0.27 | 0.29 | 0.25 | 0.23 | 0.24 | 0.15 |
| 2.01 × 1.0 | 0.53 | 0.50 | 0.65 | 0.24 | 0.28 | 0.26 | 0.23 | 0.23 | 0.09 |
| 2.56 × 1.0 | 0.58 | 0.55 | 0.73 | 0.24 | 0.26 | 0.22 | 0.18 | 0.19 | 0.05 |
| One-way drawn samples (drawn at 95°C) | | | | | | | | | |
| 1.51 × 1.0 | 0.48 | 0.44 | 0.60 | 0.30 | 0.28 | 0.28 | 0.22 | 0.27 | 0.12 |
| 1.75 × 1.0 | 0.50 | 0.47 | 0.63 | 0.26 | 0.29 | 0.25 | 0.24 | 0.24 | 0.12 |
| 1.93 × 1.0 | 0.53 | 0.49 | 0.66 | 0.27 | 0.28 | 0.24 | 0.19 | 0.23 | 0.10 |
| 2.38 × 1.0 | 0.57 | 0.53 | 0.73 | 0.24 | 0.27 | 0.20 | 0.19 | 0.21 | 0.07 |
| Simultaneously biaxially drawn samples (drawn at 85°C) | | | | | | | | | |
| 1.53 × 1.53 | 0.41 | 0.41 | 0.51 | 0.33 | 0.35 | 0.33 | 0.27 | 0.24 | 0.17 |
| 1.79 × 1.79 | 0.42 | 0.41 | 0.55 | 0.34 | 0.38 | 0.36 | 0.24 | 0.20 | 0.10 |
| Simultaneously biaxially drawn samples (drawn at 95°C) | | | | | | | | | |
| 1.46 × 1.47 | 0.40 | 0.40 | 0.52 | 0.33 | 0.37 | 0.30 | 0.27 | 0.23 | 0.18 |
| 1.66 × 1.70 | 0.40 | 0.42 | 0.48 | 0.31 | 0.36 | 0.24 | 0.28 | 0.22 | 0.28 |
| Sequentially biaxially drawn samples (drawn at 85°C) | | | | | | | | | |
| 1.53 × 1.53 | 0.39 | 0.42 | 0.51 | 0.32 | 0.35 | 0.29 | 0.29 | 0.22 | 0.20 |
| 1.79 × 1.79 | 0.42 | 0.44 | 0.55 | 0.34 | 0.36 | 0.33 | 0.24 | 0.21 | 0.13 |
| Sequentially biaxially drawn samples (drawn at 95°C) | | | | | | | | | |
| 1.51 × 1.51 | 0.40 | 0.43 | 0.51 | 0.31 | 0.35 | 0.25 | 0.29 | 0.22 | 0.24 |
| 1.64 × 1.64 | 0.42 | 0.42 | 0.52 | 0.36 | 0.36 | 0.21 | 0.36 | 0.22 | 0.21 |

determined using equations (9) to (11), and the results for the one-way and two-way drawn samples are shown in *Table 7*.

## DISCUSSION

### *Uniaxial samples*

*Birefringence data.* The samples were drawn above the glass transition temperature, which was found to lie between 71 and 82°C for all the drawn uniaxial samples. It would therefore be expected that the drawing process could be modelled in terms of the drawing of a rubber network. Rubber-like behaviour has indeed been demonstrated up to draw ratios of 2.5 for similar materials in a related set of experiments undertaken by Sweeney and Ward[26]. It was found that the stress could be modelled in terms of an Ogden-type strain-energy function and that the strain was fully recoverable up to at least this draw ratio. The value of the exponent of $\lambda$ required in the Ogden function was less than 2, which is expected on the basis of the simple Gaussian rubber network with constant crosslink density. The birefringence data shown in *Figure 1* are in excellent agreement with similar data obtained by Jabarin[7] for the same range of draw temperatures, but they do not fit the simple Gaussian theory; on that theory the curves would be convex to the draw ratio axis, unlike the experimental curves shown in *Figure 1*. The effective crosslinks are crystallites, and entanglements and deviations may be due to a reduction in the effective crosslink density with increasing draw ratio in a manner analogous to that suggested by Raha and Bowden[27] for poly(methyl methacrylate). The lower birefringence observed at a given draw ratio as the draw temperature is raised could be explained by a reduction in the effective crosslink density with increasing temperature for a given draw ratio.

*Infra-red data.* The peaks at 607 and 639 $cm^{-1}$ have previously been assigned to crystalline syndiotactic chain segments, the peak at 613 $cm^{-1}$ to short non-crystalline syndiotactic planar zig-zag chain segments and the peak at 689 $cm^{-1}$ to the isotactic helical conformation[6,21]. If it is assumed that the extinction coefficients are the same per chlorine atom for all the absorbance peaks in the $\nu$CCl region, the crystallinity can be estimated as the fraction of the total equivalent isotropic absorbance contributed by the two peaks at 607 and 639 $cm^{-1}$. The isotropic absorbance is obtained as one-third of the result of adding the parallel absorbance to twice the perpendicular absorbance. *Table 6* shows that the crystallinities calculated in this way are somewhat higher than those generally found for commercial PVC ($\sim 10\%$), so that the absolute values may not be correct. Nevertheless, the suggested small rise in crystallinity with draw temperature is probably correct; the small fall with draw ratio is less certain.

One of the reasons for questioning the absolute values of crystallinity, in addition to the fact that the extinction coefficients for the different $\nu$CCl frequencies may not be equal, is that vinyl acetate has a peak in the 607 $cm^{-1}$ region and this may not have been correctly allowed for. For this second reason, the values of $\langle P_2(\cos\theta)\rangle$ derived from the absorbances for the 607 $cm^{-1}$ peak are likely to be less accurate than those derived from the absorbances for the other peaks. The data in *Table 5* show that the correction for additives has no significant effect on the values of $\langle P_2(\cos\theta)\rangle$ deduced from the peaks at 613 and 689 $cm^{-1}$, and only a small effect for the peak at 639 $cm^{-1}$, whereas it has a larger effect for the peak at 607 $cm^{-1}$. *Table 6* and *Figure 5* show that the orientation of the crystalline material is higher for a higher temperature of draw at a given draw ratio, in contrast to the reduced overall orientation with increasing temperature indicated by the birefringence. This result, which agrees with what was found previously[2], may possibly be accounted for by the increased mobility of the amorphous phase at higher temperature allowing the crystallites, which are probably fibrillar in nature, to rotate further towards their preferred orientation during drawing, while permitting greater relaxation in the amorphous regions. The increase in crystallinity observed at higher temperatures of drawing is probably due to the thermal equilibration of the sample before drawing.

The orientation of the short syndiotactic segments, deduced from the absorbances at 613 $cm^{-1}$, is lower than that of the crystalline material (see *Table 6*). This contrasts with the results found previously using Raman spectroscopy[3] for a series of plasticized samples drawn at temperatures of 90°C or lower, where the short syndiotactic sequences were found to orient in a very similar manner to the crystallites. It will be assumed tentatively that the orientation of the short syndiotactic

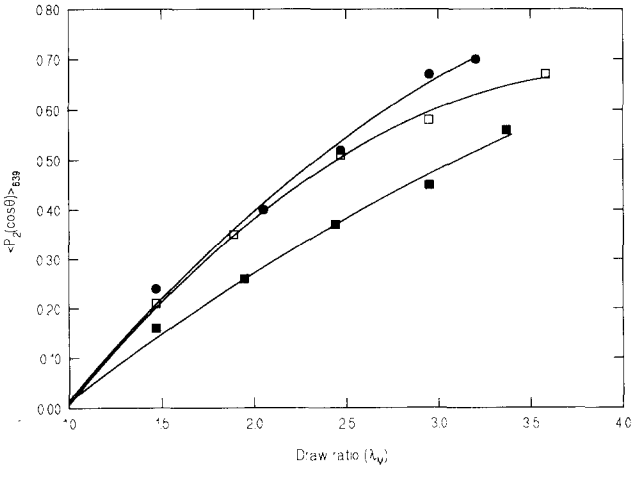


**Figure 5** Dependence of $\langle P_2(\cos\theta)\rangle$ values obtained from the 639 $cm^{-1}$ i.r. peak on draw ratio $\lambda_M$. Notation as in *Figure 1*

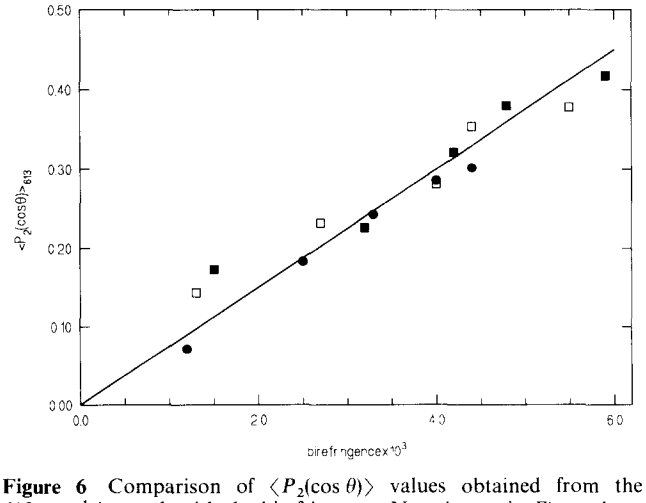


**Figure 6** Comparison of $\langle P_2(\cos\theta)\rangle$ values obtained from the 613 $cm^{-1}$ i.r. peak with the birefringence. Notation as in *Figure 1*

sequences is a measure of the orientation of the non-crystalline material.

*Figure 6* shows that the values of $\langle P_2(\cos\theta)\rangle$ derived from the 613 $cm^{-1}$ peak are approximately proportional to the birefringence, independently of the draw temperature. This is, at first sight, difficult to reconcile with the assumption just made, since the dependence of crystalline orientation on draw temperature for a given overall orientation implies a dependence on draw temperature for the non-crystalline orientation for a given overall orientation. The crystallinity is, however, rather low, and the temperature dependence not great.

The values of $\langle P_2(\cos\theta)\rangle$ for the crystalline and non-crystalline material, derived from the data for the 639 and 613 $cm^{-1}$ absorptions, can in fact be combined with the crystallinity determined from the 607 and 639 $cm^{-1}$ absorptions to deduce the values of the overall orientation average $\langle P_2(\cos\theta)\rangle_{av}$. *Figure 7* shows that when these values are plotted against the birefringence, a fairly good straight line relationship passing through the origin is found, with the gradient independent of the drawing temperature. Extrapolation of the least-squares fitted line of *Figure 7* to $\langle P_2(\cos\theta)\rangle_{av}=1$ leads to the value $12.5\times10^{-3}$ for the birefringence of a fully oriented sample. This is close to the values $12.6\times10^{-3}$ and $13.0\times10^{-3}$ found previously by n.m.r.[8] and Raman[2] spectroscopy, respectively, for uniaxially oriented PVC. Since the present samples contain vinyl acetate and other additives, it is surprising that the values agree as well as they do. The agreement does, however, support the assumption that the orientation average deduced from the peak at 613 $cm^{-1}$ is a measure of the orientation of the non-crystalline material and the assumption made in the calculations that the dipole moment for this absorption lies fairly close to the normal to the chain axis.

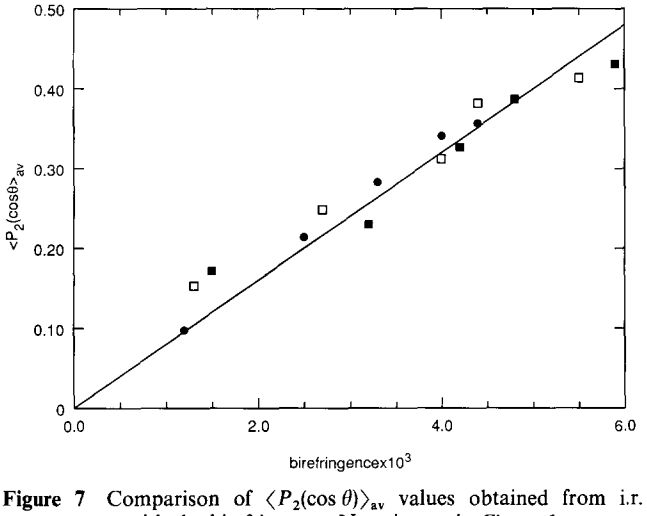


**Figure 7** Comparison of $\langle P_2(\cos\theta)\rangle_{av}$ values obtained from i.r. spectroscopy with the birefringence. Notation as in *Figure 1*

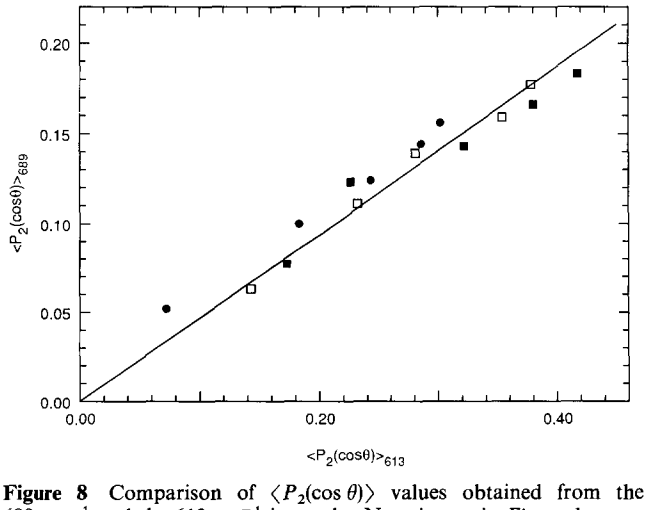


**Figure 8** Comparison of $\langle P_2(\cos\theta)\rangle$ values obtained from the 689 $cm^{-1}$ and the 613 $cm^{-1}$ i.r. peaks. Notation as in *Figure 1*

*Figure 8* shows a plot of $\langle P_2(\cos\theta)\rangle$ deduced from the absorbances for the 689 $cm^{-1}$ peak against that for the 613 $cm^{-1}$ peak. Since both peaks are due to amorphous material, a straight line relationship independent of draw temperature might be anticipated, as found. It is not possible to predict the gradient of the line, since the orientation of the absorption dipole for the 689 $cm^{-1}$ peak is not known. In practice it shows perpendicular dichroism and the calculations were made assuming a dipole perpendicular to the chain axis. The results show that either this is incorrect or the corresponding segments are less well oriented than the syndiotactic segments or, more probably, that both of these effects are present.

Jabarin[7] assumed that the absorption at 690 $cm^{-1}$, which we have shown to be composed of several components, could be used to derive the values of $\langle P_2(\cos\theta)\rangle$ for the non-crystalline material, taking the transition dipole to be perpendicular to the chain axis. He found that there was a linear relationship between the values of $\langle P_2(\cos\theta)\rangle$ so obtained and the birefringence, and deduced a value of $20.3\times10^{-3}$ for the birefringence of a fully oriented amorphous sample. This value is necessarily higher than that evaluated above, because of the low orientation values found from the 690 $cm^{-1}$ peak. The values given by the present data for the 689 $cm^{-1}$ peak are even lower than those of Jabarin for a given birefringence. This difference probably arises because he does not appear to have used curve resolution to separate the observed peak at 690 $cm^{-1}$ into its constituent components, as done here. It seems in any case unlikely that the values of $\langle P_2(\cos\theta)\rangle$ determined from the peak at 690 $cm^{-1}$ should adequately represent the orientation of the amorphous material, since the peak is assigned to chlorine atoms at points where the chain is not in its planar zig-zag form, so that the definition of a chain axis is ambiguous, in addition to the uncertainty in the orientation of the transition dipole.

*Elastic moduli. Figure 9* shows the 10 s creep moduli plotted against birefringence for the present samples and for samples studied previously[4], which were drawn at 70°C at a draw speed of 1 cm $min^{-1}$ from PVC containing 4 parts by weight of stabilizer per 100 parts of polymer or containing 4 parts of stabilizer and 5 parts of plasticizer by weight per 100 parts of polymer. Each series of samples exhibits a similar dependence of modulus on overall orientation, though the absolute values of the moduli are lower for the present series of samples than for the previous series. It was shown in the earlier work that the difference in modulus between the plasticized and unplasticized samples could be accounted for in terms of a dilution effect of the plasticizer, and the difference between the present and previous samples can probably be attributed to a similar effect, with a larger fraction of additives. The small differences observed with

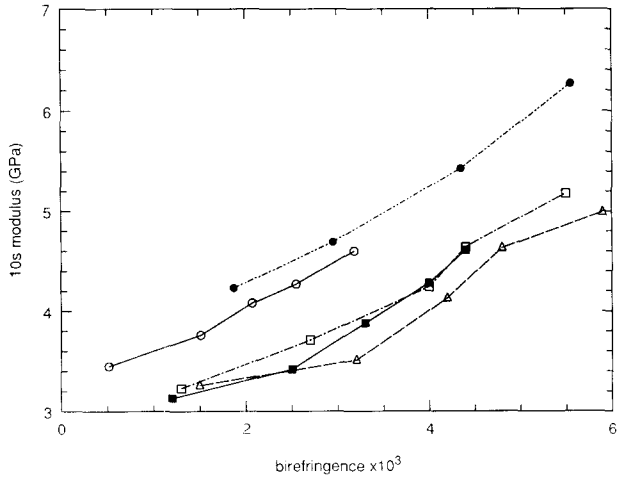


**Figure 9** Comparison of 10 s modulus obtained from the uniaxially oriented samples with the birefringence: ●, unplasticized[3]; ○, plasticized[3]. $T_d$ value: ■, 110°C; □, 100°C; △, 90°C

draw temperature for the present samples are not sufficiently systematic to be meaningful.

For a given draw temperature the dynamic storage moduli show a slightly smaller temperature dependence as the overall orientation of the samples increases. This is probably the result of the greater crystallinity and greater crystal orientation of the samples drawn at higher temperature.

*One-way and two-way drawn samples*

These samples were drawn close to or just above their final glass transition temperatures. *Table 7* shows the values of the averages $\langle \cos^2 \theta_{c,i} \rangle$ deduced from the i.r. data for the peaks at 613 and 639 $cm^{-1}$, and from the refractive indices (optical). As expected, the optical values are close to the values obtained from the peak at 613 $cm^{-1}$, particularly for the one-way drawn samples. The comparisons between the various values are more easily seen in the equilateral triangular plots in *Figures 10* and *11*. In these figures the value of $\langle \cos^2 \theta_{c,i} \rangle$ is proportional to the perpendicular distance of the corresponding point from the side of the triangle opposite to the vertex *i*. The figures show that the one-way drawn samples are not uniaxial but show a tendency for their chain axes to be oriented preferentially towards the plane of the film, although this tendency is very slight except for the crystalline chains. *Table 7* and *Figures 10* and *11* also show that there is no evidence for a difference in the type of orientation produced by simultaneous and sequential biaxial stretching, unlike that observed for isotactic polypropylene[18]. The orientation of the present samples is, however, much lower than that observed for polypropylene.

There is a clear tendency for the chains in the biaxially oriented samples to orient towards the plane of the film, but the corresponding points in *Figures 10* and *11* do not lie on the line representing uniaxial distributions with respect to the normal direction. This is because the starting material was not completely unoriented, as shown by the refractive indices for the undrawn material in *Table 2*. These values, which were obtained after subjecting the samples to the same preheating as the drawn samples, show that the starting material was slightly uniaxially oriented towards the machine direction.

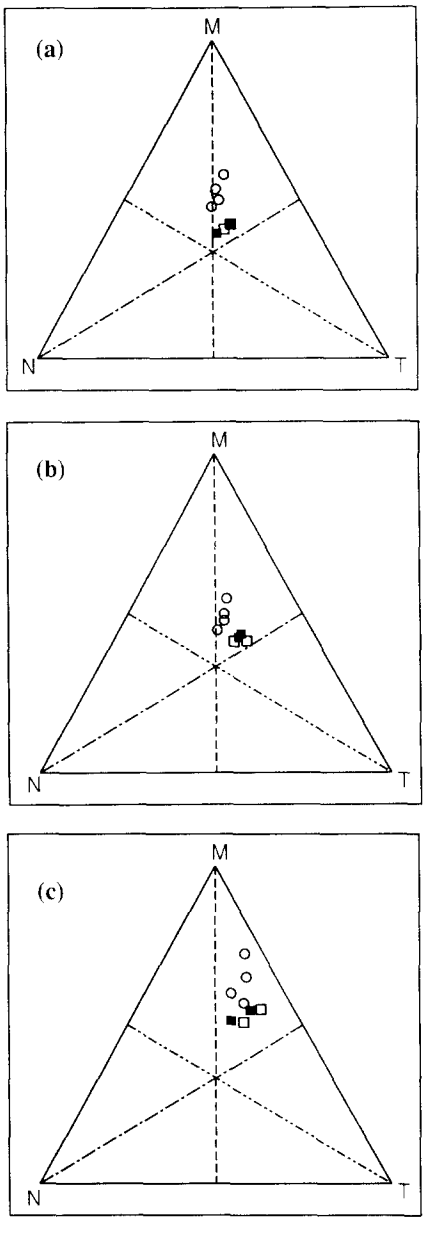


**Figure 10** Equilateral triangular plots of $\langle \cos^2 \theta_{c,i} \rangle$ ($i$ = M, N or T) values obtained from the one-way and sequentially and simultaneously biaxially oriented samples drawn at 85°C: (a) for amorphous chains, obtained from the 613 $cm^{-1}$ i.r. peak; (b) for all chains, calculated from the refractive indices; (c) for crystalline chains, obtained from the 639 $cm^{-1}$ i.r. peak. ○, One-way drawn; □, simultaneously two-way drawn; ■, sequentially two-way drawn

The observed orientation of the biaxially drawn samples is clearly consistent with a starting point slightly above the random points in the figures.

There is little difference in the degree of orientation produced at the two draw temperatures, though there appears to be a tendency for the crystalline chains in the biaxially oriented films to remain uniaxially oriented towards the machine direction at the higher draw temperature.

## CONCLUSIONS

A combination of refractive index and i.r. measurements on a series of uniaxially oriented samples of PVC has enabled an estimate to be made of the maximum

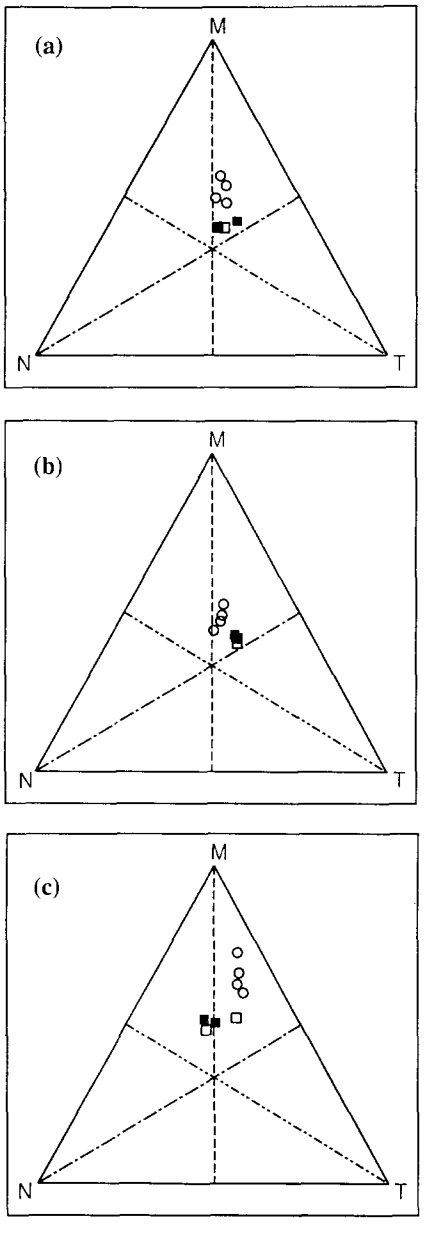


**Figure 11** Equilateral triangular plots of $\langle \cos^2 \theta_{c,i} \rangle$ ($i$ = M, N or T) values obtained from the one-way and sequentially and simultaneously biaxially oriented samples drawn at 95°C: (a) for amorphous chains, obtained from the 613 $cm^{-1}$ i.r. peak; (b) for all chains, calculated from the refractive indices; (c) for crystalline chains, obtained from the 639 $cm^{-1}$ i.r. peak. Notation as in *Figure 10*

birefringence for a fully uniaxially oriented sample. This value has been used to deduce orientation averages for one-way and two-way drawn samples from their refractive indices for comparison with values deduced from i.r. data. The results show that one-way drawn samples depart slightly from uniaxiality. No significant difference in orientation was found between simultaneously and sequentially two-way drawn samples. It was shown that the i.r. peak at 613 $cm^{-1}$, attributed to short syndiotactic segments, could be used to characterize the orientation of the amorphous chains. The elastic moduli of the uniaxially drawn samples were found to depend on orientation in a similar way to that reported previously.

## ACKNOWLEDGEMENTS

The authors thank ICI plc for donating the starting materials, Dr J. Sweeney for help in preparing the oriented samples, and a referee for useful comments.

## REFERENCES

1 Selwood, A., Taraiya, A. K. and Ward, I. M. *Plast. Rubber Process Applic.* 1988, **10**, 85
2 Robinson, M. E. R., Bower, D. I. and Maddams, W. F. *J. Polym. Sci., Polym. Phys. Edn* 1978, **16**, 2115
3 Bower, D. I., King, J. and Maddams, W. F. *J. Macromol. Sci. Phys.* 1981, **B20**(3), 305
4 King, J., Bower, D. I. and Maddams, W. J. *J. Appl. Polym. Sci.* 1988, **35**, 787
5 Shindo, Y., Read, B. E. and Stein, R. S. *Makromol. Chem.* 1968, **118**, 272
6 Theodorou, M. and Jasse, B. *J. Polym. Sci., Polym. Phys. Edn* 1986, **24**, 2643
7 Jabarin, S. A. *Polym. Eng. Sci.* 1991, **31**, 638
8 Kashiwagi, M. and Ward, I. M. *Polymer* 1972, **13**, 145
9 Vyvoda, J. C., Gilbert, M. and Hemsley, D. A. *Polymer* 1980, **21**, 109
10 Liu, Z. and Gilbert, M. *Polymer* 1987, **28**, 1303
11 Brady, T. E. *Polym. Eng. Sci.* 1976, **16**, 638
12 de Vries, A. J. and Bonnebat, C. *Polym. Eng. Sci.* 1976, **16**, 93
13 Sakaguchi, K. and Nagano, I. *Bull. Jap. Soc. Mech. Eng.* 1986, **29**, 2426
14 Sakaguchi, K. and Nagano, I. *Bull. Jap. Soc. Mech. Eng.* 1986, **29**, 4454
15 Gilbert, M. and Liu, Z. *Plast. Rubber Process Applic.* 1988, **9**, 67
16 Gupta, V. B. and Ward, I. M. *J. Macromol. Sci. Phys.* 1967, **B1**, 373
17 Lewis, E. L. V. *J. Mater. Sci.* 1979, **14**, 2343
18 Karacan, I., Taraiya, A., Bower, D. I. and Ward, I. M. *Polymer* 1993, **34**, 2691
19 Green, D. I. and Bower, D. I. *Spectrochem. Acta* 1993, **49A**, 1191
20 Jackson, R. S., Bower, D. I. and Maddams, W. F. *J. Polym. Sci., Polym. Phys. Edn* 1990, **28**, 837
21 Bower, D. I. and Jackson, R. S. *J. Polym. Sci., Polym. Phys. Edn* 1990, **28**, 1589
22 Maddams, W. F. and Tooke, P. B. *J. Macromol. Sci.-Chem.* 1982, **A17**(6), 951
23 Jarvis, D. A., Hutchinson, I. J., Bower, D. I. and Ward, I. M. *Polymer* 1980, **21**, 41
24 Cunningham, A., Davies, G. R. and Ward, I. M. *Polymer* 1974, **15**, 743
25 Cunningham, A., Ward, I. M., Willis, H. A. and Zichy, V. *Polymer* 1974, **15**, 749
26 Sweeney, J. and Ward, I. M. *Trans. Inst. Chem. Eng. Part A* 1993, **71**, 232
27 Raha, S. and Bowden, P. B. *Polymer* 1972, **13**, 174
28 Pohl, H. U. and Hummel, D. O. *Makromol. Chem.* 1968, **113**, 190, 203
29 Theodorou, M. and Jasse, B. *J. Polym. Sci., Polym. Phys. Edn* 1983, **21**, 2263